Surfactant Boundary Lubricant Film Modified by an Amphiphilic Diblock Copolymer

ARTICLE *in* LANGMUIR · APRIL 2005

Impact Factor: 4.46 · DOI: 10.1021/la047878e · Source: PubMed

5 AUTHORS, INCLUDING:

Annabelle Blom
BHPBilliton, Olympic Dam
10 PUBLICATIONS **101** CITATIONS
SEE PROFILE

Erica J Wanless
University of Newcastle
81 PUBLICATIONS **2,514** CITATIONS
SEE PROFILE

Gregory G Warr
University of Sydney
189 PUBLICATIONS **5,002** CITATIONS
SEE PROFILE

Surfactant Boundary Lubricant Film Modified by an Amphiphilic Diblock Copolymer

A. Blom,[†] C. Drummond,[‡] E. J. Wanless,[§] P. Richetti,*[,‡] and G. G. Warr[†]

School of Chemistry, F11, University of Sydney, NSW 2006, Australia, Centre de Recherche Paul Pascal, Avenue Schweitzer, Pessac 33600, France, and School of Environmental and Life Sciences, University of Newcastle, Callaghan, NSW 2308, Australia

Received August 25, 2004. In Final Form: December 7, 2004

The effect of the uptake of a low-molecular-weight amphiphilic diblock copolymer on the morphology of didodecyldimethylammonium bromide (DDAB) adsorbed layers on mica, the interactions between two coated surfaces, and the frictional properties of the boundary film have been studied using an atomic force microscope and a dynamic surface forces apparatus nanotribometer. When DDAB-coated surfaces in aqueous solution were compressed, hemifusion or removal of the adsorbed surfactant bilayers could not be induced, and no frictional force could be measured between the surfaces, which display superior lateral cohesion and lubricant properties. Coadsorbing octadecyl end modified poly(ethylene oxide) chains at low density facilitates hemifusion, generating significant shear stress and leading to stick−slip instabilities. The mixed films regain their lateral cohesion at higher adsorbed copolymer densities, but an extra short-range attraction brings the adsorbed layers into adhesive contact without causing bilayer hemifusion. Here, noticeable frictional forces are also measured.

Introduction

In both natural and engineered applications the use of surfactants and polymers to reduce or control friction is widespread.[1] There is a particular need to develop an understanding of water-based lubricants for biomedical and environmentally friendly applications. Water-based lubricants facilitate the sliding of proximate surfaces through a variety of mechanisms including steric or electrostatic repulsion and surface hydration. Ultimately, a boundary lubricant film should exhibit relatively weak friction forces in comparison to the unlubricated system. Smooth sliding of the rubbed surfaces is also desirable in order to avoid high accelerations that might increase the rate of dissipation of energy and the probability of irreversible wear and surface damage.

The investigation of the frictional properties has progressed greatly over the past 20 years owing to the application of direct lateral force measurement. Surfactant films deposited or self-assembled from solution have been demonstrated to modify the frictional characteristics of solid substrates in air, and to depend on many parameters such as temperature, pressure, humidity, sliding velocity, and density of the deposited layers,[2] as well as intrinsic characteristics of the surfactant investigated such as chain length, degree of unsaturation, and endgroup functionality.[3]

Of perhaps greater impact are the frictional characteristics of surfaces immersed in aqueous surfactant solutions. It has been shown that charged surfactants that self-assemble on surfaces may be very effective boundary lubricants.[4] Due to the electrostatic repulsion between the adsorbed layers, the friction force between coated surfaces is extremely low, as long as the layers adsorbed on the rubbing surfaces remain undamaged. Disruption of the adsorbed layer leads to more complicated shear behavior, particularly if the adsorbed bilayers hemifuse. Several dynamic regimes may then be observed, depending on the relative velocity of the rubbed surfaces and the experimental conditions.[4−6] In particular, an inverted stick−slip regime bounded by smooth sliding regimes as the sliding velocity varies has been observed in aqueous solutions of CTAC, the gemini surfactant 12-3-12, and a trimeric equivalent, 12-3-12-3-12. This behavior can then be described in terms of an adhesive−viscous model, based on the kinetics of formation and rupture of adhesive links with an added viscous term.[4−6]

Adsorption of polymer brushes has also been demonstrated to dramatically reduce the effective friction coefficient between mica surfaces in toluene under good solvent conditions.[7] This was attributed to a long-ranged entropic repulsion acting to maintain a finite surface separation with a relatively fluid intervening film. Further studies[8,9] have shown that end-tethered polymer chains are much less effective lubricants in near-θ solvents, due to weaker excluded volume repulsions and higher entanglement between the brushes.

Among the polymers studied, poly(ethylene oxide), PEO, belongs to a class of its own. This water-soluble polymer is known for its low toxicity, and has been extensively used in coatings of implant devices to reduce protein adsorption, protect against bacterial growth, and enhance

* Corresponding author. E-mail: richetti@crrp-bordeaux.cnrs.fr.
[†] Univesity of Sydney.
[‡] Centre de Recherche Paul Pascal.
[§] University of Newcastle.

(1) Persson, B. N. J. *Sliding friction: Physical principles and applications.*; Springer: Heidelberg, 1998.
(2) Yoshizawa, H.; Chen, Y. L.; Israelachvili, J. *J. Phys. Chem.* **1993**, *97*, 4128.
(3) Liu, Y.; Evans, D. F.; Song, Q.; Grainger, D. W. *Langmuir* **1996**, *12*, 1235.
(4) Richetti, P.; Drummond, C.; Israelachvili, J.; In, M.; Zana, R. *Europhys. Lett.* **2001**, *55*, 653.
(5) Drummond, C.; Israelachvili, J.; Richetti, P. *Phys. Rev. E* **2003**, *67*, 066110.
(6) Drummond, C.; Elezgaray, J.; Richetti, P. *Europhys. Lett.* **2002**, *58*, 503.
(7) Klein, J.; Kumacheva, E.; Mahalu, D.; Perahia, D.; Fetters, L. J. *Nature* **1994**, *370*, 634.
(8) Schorr, P. A.; Kwan, T. C. B.; Kilbey, S. M., II; Shaqfeh, E. S. G.; Tirrell, M. *Macromolecules* **2003**, *36*, 389.
(9) Granick, S.; Demirel, A. L.; Cai, L. L.; Peanasky, J. *Isr. J. Chem.* **1995**, *35*, 75.

10.1021/la047878e CCC: $30.25
Published on Web 03/02/2005

biocompatibility.[10] Several studies of grafted, end-modified PEO molecules under shear have been reported.[11,12] Raviv et al.[11] observed that interpenetration between the opposing layers and bridging affect the frictional forces between mica surfaces bearing trimethylammonium-terminated poly(ethylene oxide) brushes in aqueous media.

Fewer studies have addressed the behavior of surfactant/polymer mixtures as boundary lubricants. In an earlier study combining atomic force microscopy (AFM) and surface forces apparatus (SFA) measurements,[13] we demonstrated the anchoring or tethering of three low-molecular-weight block copolymers into the adsorbed layer of dodecyltrimethylammonium bromide (DTAB) on mica, although the copolymers alone did not adsorb on this substrate. One of these copolymers consisted of an octadecyl hydrophobic block and 100 oxyethylene units as the hydrophilic block, denoted D100. The hydrophobic block is incorporated in the surface aggregates of the DTAB on mica, modifying the rodlike morphology[14] of the adsorbed surfactant and inducing a transition to globular aggregates above 0.18 wt % copolymer. In a separate study with 12-3-12-3-12 trimeric surfactant, we showed how the coadsorption of D100 diblock copolymer on the preadsorbed surfactant bilayer affects the surfaces under shear.[15]

We report here on the effect of coadsorbing D100 into a bilayer of the surfactant didodecyldimethylammonium bromide (DDAB), and we investigate whether D100 can modify the morphology of the adsorbed flat layer, as well as the consequences for interactions between such coated surfaces. Both an AFM and a modified-SFA have been employed: the former to monitor the lateral homogeneity and the morphology of the adsorbed layer, and the latter to obtain precise measurements of interlayer interactions both normal and under shear.

Experimental Section

Materials. Didodecyldimethylammonium bromide (DDAB; Fluka) was purchased as a 99% pure sample and used as received. DDAB forms vesicles in aqueous solution at concentrations above 10^{-4} M,[16] and adsorbs on mica as a bilayer that is laterally homogeneous as determined by soft-contact atomic force microscopy.[17,18]

Myrj 59 (D100), a polydisperse polyoxyethylene 100 stearate ($C_{18}E_{100}$), was purchased from Aldrich and used as received. This commercial diblock copolymer self-assembles as micelles in water at very low concentrations (cmc < 10^{-5} M), and forms mixed micelles with ionic surfactants in bulk solution. The purity of the product was verified by NMR and by size-exclusion chromatography (SEC). The measured polydispersity index M_w/M_n was 1.15.

Ground muscovite mica was obtained from Brown & Co., Sydney, and used as received. All experiments were performed at room temperature, 23 °C, unless otherwise stated.

Methods. *Depletion Experiments.* The composition of the mixed DDAB/D100 adsorbed films at the mica surface were measured by equilibrating 18.5 mL of 1 mM DDAB and D100 solutions with 1.5 g of ground mica. Solutions were equilibrated for 3 days on a roller mixer (Ratek BTR5, Ratek Instruments) and then centrifuged at 8000 rpm (Hettich Universal centrifuge) for 5 min. The supernatant was separated by HPLC (Waters), and concentrations of DDAB and D100 remaining in solution were analyzed using a differential refractometer (Waters 2410). The column used was a Symmetry C18 column (Waters) operating with Empower Pro software, and the eluent used was 90:10 methanol to water with 0.2 M NaCl.

Atomic Force Microscopy. Adsorbed layer structures at the solid/solution interface were examined using a Digital Instruments NanoScope IIIa Multimode atomic force microscope in contact mode in a standard fluid cell. Standard cantilevers were used with sharpened Si_3N_4 tips (Digital Instruments). These were irradiated with ultraviolet light for 30 min prior to use. The solution was held in a fluid cell and sealed by a silicone O-ring. Both were cleaned by sonication for 10 min in the surfactant solution to be studied, rinsed in ethanol and deionized water, and then dried using filtered nitrogen. The solid substrate used in all experiments was muscovite mica (Probing and Structure, Queensland). The mica substrate was cleaved using adhesive tape immediately before use. Experiments were performed in Millipore water with a conductivity of 18 MΩ cm^{-1}.

Images shown display deflection data captured using a soft contact method[18] in which surfactant adsorption on both the tip and the substrate allows imaging using electrical double layer forces. This method enables generation of a double-layer force map of the adsorbed layer without the tip physically contacting the sample. Typical imaging scan rates varied between 8 and 15 Hz, and integral gains between 0.8 and 1 were used. Variation of frequency, scan angle, and gains had no effect on the observed morphology. All images are unmodified except for flattening along scan lines.

Force versus separation experiments were performed on a single 200 μm long cantilever. In converting the measured cantilever deflection into force, the manufacturer-provided spring constant of 0.32 N/m and radius of 0.02 μm were used. These nominal values of spring constant and radius may not be correct, but no attempt was made to measure the actual values. However, this does not affect the relative intensity of the force measured with the same tip in the different systems investigated.

Surface Forces Apparatus (SFA). A Surface forces apparatus (SFA) modified for nanotribological studies[19] was used to measure the interaction between surfactant−polymer coated mica surfaces. This technique has been extensively described in the past. In brief, two back-silvered molecularly smooth mica surfaces are glued to cylindrically curved silica lenses. With the SFA it is possible to study a single asperity contact, owing to the molecular smoothness of cleaved mica surfaces and the crossed-cylinder configuration used. The separation between the surfaces can be controlled with an accuracy of a fraction of a nanometer by using a piezoelectric nanopositioner. Multiple beam interferometry (MBI) is used to measure the separation between the surfaces, D, with subnanometric resolution, their local radius of curvature, R, and the refractive index of the confined film.[20] The force−distance profile between the surfaces is measured by changing the position of the double cantilever spring attached to the lower surface, and measuring by MBI the actual variation in the separation between the surfaces. The interaction force is then determined from the deflection of the spring by using Hooke's law. If a normal force, L, is applied to the surfaces in contact, the cylinders are elastically flattened at the point of contact. The load-induced contact radius of a few tens of micrometers, R_c, and the area of contact, A, can be directly measured by MBI.

We are able to induce a lateral relative motion between the surfaces by voltage-driven bimorph strips attached to the lower surface.[21] Shearing cycles are carried out by moving this surface at constant velocity, V, over a certain distance, after which the driving direction is reversed. The upper surface is attached to a vertical double cantilever spring whose deflection is monitored using strain gauges (SurForce Inc). The friction force, F_f, induced by the relative displacement between the surfaces in contact can then be calculated from the experimentally measured spring force, F_s, obtained from the deflection of this double cantilever spring, with an accuracy of ±5 μN.

(10) Elbert, D. L.; Hubbell, J. A. *Annu. Rev. Mater. Sci.* **1996**, *26*, 365.
(11) Raviv, U.; Frey, J.; Sak, R.; Laurat, P.; Tadmor, R.; Klein, J. *Langmuir* **2002**, *18*, 7482.
(12) Zhang, X.; Granick, S. *Macromolecules* **2002**, *35*, 4017.
(13) Robelin, C.; Duval, F. P.; Richetti, P.; Warr, G. G. *Langmuir* **2002**, *18*, 1634.
(14) Patrick, H. N.; Warr, G. G.; Manne, S.; Aksay, I. A. *Langmuir* **1999**, *15*, 1685.
(15) Drummond, C.; In, M.; Richetti, P. *Eur. Phys. J. E* **2004**, *15*, 159.
(16) Warr, G. G.; Grieser, F. *Chem. Phys. Lett.* **1984**, *116*, 505.
(17) Manne, S.; Gaub, H. E. *Science* **1995**, *270*, 1480.
(18) Manne, S.; Cleveland, J. P.; Gaub, H. E.; Stucky, G. D.; Hansma, P. K. *Langmuir* **1994**, *10*, 4409.
(19) Homola, A.; Israelachvili, J. N.; Gee, M. L.; McGuiggan, P. *J. Tribol.* **1989**, *111*, 675.
(20) Israelachvili, J. N. *J. Colloid Interface Sci.* **1973**, *44*, 259.
(21) Luengo, G.; Schmitt, F. J.; Hill, R.; Israelachvili, J. *Macromolecules* **1997**, *30*, 2482.

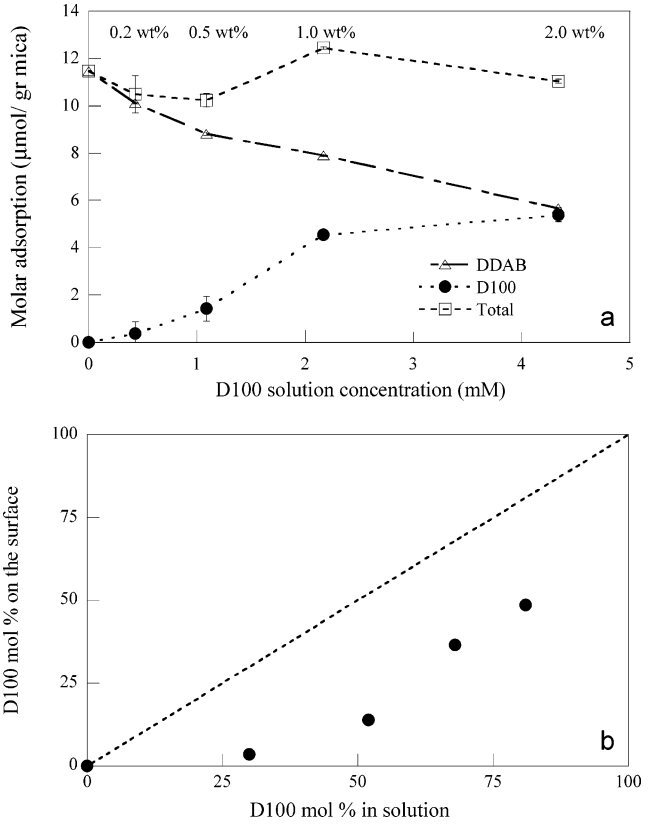

Figure 1. Adsorption of DDAB/D100 mixtures at mica−water interface. (a) Adsorbed amounts of DDAB, D100, and total adsorbed amounts for 1 mM DDAB, 1 mM DDAB + 0.2 wt % D100 (0.43 mM), 1 mM DDAB + 0.5 wt % D100 (1.1 mM), 1 mM DDAB + 1 wt % D100 (2.2 mM), and 1 mM DDAB + 2 wt % D100 (4.3 mM). (b) Variation of amount of D100 adsorbed with concentration of D100 in solution. The 1:1 line shows the behavior expected for ideally mixed components.

The mica surfaces were exposed to the DDAB−D100 solution of interest at least 16 h before the measurements, to achieve what we believe was the thermodynamic equilibrium state of the self-assembled layers.

Results

Adsorption. Figure 1 shows the measured adsorption of DDAB and D100 on the surface of ground mica for several D100 bulk polymer concentrations. The DDAB concentration was 1 mM in all cases. The highest polymer concentration investigated was 2 wt %, as the DDAB−D100 solutions phase separated at higher concentrations. As Figure 1a shows, increasing the ratio D100/DDAB in solution increases the fraction of D100 in the mixed adsorbed layer while the total adsorbed amount (DDAB + D100) remains approximately constant. The same data are presented in Figure 1b, as mole fraction of adsorbed D100 versus its mole fraction in solution. As can be observed, uptake of D100 is much less than the 1:1 ratio expected from ideal adsorption, shown as the diagonal line in Figure 1b. This is by no means unexpected, given the poor affinity of the D100 polymer for the mica surfaces, and the strong, electrostatically driven adsorption of the cationic surfactants onto the negatively charged mica surfaces. This indicates that the adsorption of D100 molecules occurs mainly by tethering of the hydrophobic moiety onto the adsorbed surfactant layer. Below about 0.4 wt % D100 in solution, there is little coadsorption of D100 molecules. However this increases markedly at higher concentrations and is accompanied by a substantial decrease in the amount of adsorbed DDAB.

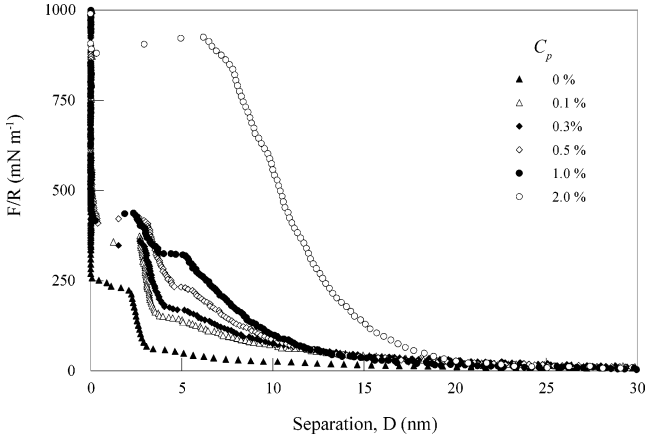

Figure 2. Normal tip−surface interaction force measured by AFM in a solution of 1 mM DDAB and 0, 0.1, 0.3, 0.5, 1, and 2 wt % D100.

Table 1. Separation and Force at Breakthrough of a DDAB Film in 1 mM Solution with Addition of D100

	separation (nm)		force (mN/m)	
copolymer loading	outer	inner	outer	inner
0 wt % (pre-DDAB)		2.1 ± 0.3		204 ± 20
0.1 wt % D100		2.7		381 ± 18
0.2 wt % D100		2.0 ± 0.1		334 ± 7
0.3 wt % D100		2.6		363 ± 11
0.5 wt % D100	5.1 ± 0.7	2.3 ± 0.2	427 ± 20	223 ± 10
1 wt % D100	5.0 ± 0.5	2.3 ± 0.3	428 ± 23	306 ± 11
2 wt % D100	6.1 ± 0.6		847 ± 70	

Atomic Force Microscope: Morphology of the Adsorbed Layer and Normal Interaction Forces. Figure 2 shows AFM force profiles for the mixed DDAB and D100 systems for different polymer concentrations between 0.1 and 2 wt %. With no added D100, the force profile obtained on a pure DDAB bilayer shows the hard wall repulsion characteristic of a bilayer resistant to compression by the tip. The position $D = 0$ was established as the mica−tip contact position, evidenced as a constant slope on the AFM deflection curve after the double layer repulsive force barrier has been overcome. The measured separation at breakthrough of 2.1 ± 0.3 nm is consistent with AFM results reported elsewhere,[17] and with a measured bilayer thickness on quartz of 2.6 nm from neutron reflectometry[22] considering compression prior to breakthrough by the AFM tip. We can distinguish two polymer concentration regimes. For polymer concentrations between 0.1 and 0.3 wt %, the film thickness is not significantly changed, although the strength of the film, indicated by the deflection at breakthrough, approximately doubles from that measured for the pure DDAB film. At a polymer concentration of 0.5 wt %, the force profile changes shape, and a second layer with a breakthrough approximately 2.8 nm further out from the original film develops. This is observed again at 1 wt % D100, with both of these curves similar in shape, measured separations, and deflections. At 2 wt % polymer, the inner breakthrough is no longer observed and only one jump into contact occurs from approximately 6.1 nm. All of these experiments were performed using a single tip. The results are summarized in Table 1.

Figure 3 shows a 300 nm × 300 nm image of 0.5 wt % D100 grafted into an adsorbed DDAB film. Figure 3a was imaged at a force corresponding to the layer furthest from the mica surface (separation ~ 5.2 nm), and Figure 3b

(22) Schulz, J. C.; Warr, G. G.; Butler, P. D.; Hamilton, W. A. *Phys. Rev. E* **2001**, *63*, 041604.

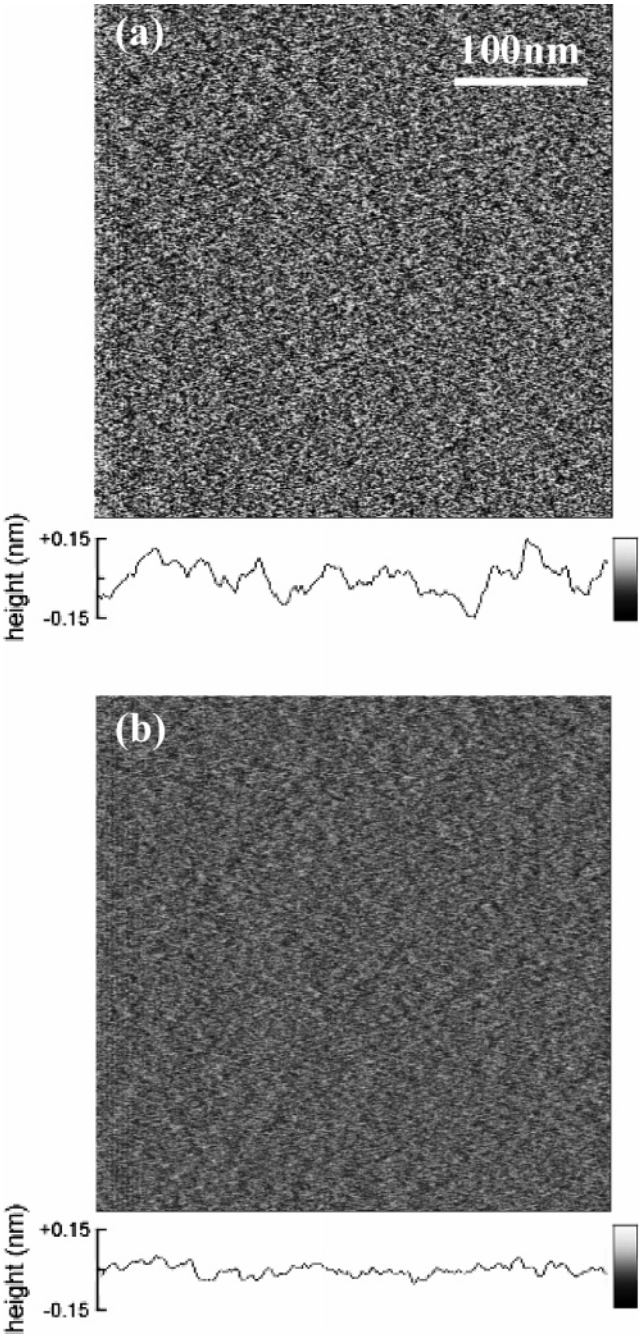

Figure 3. 300 nm × 300 nm AFM deflection images of a mixed adsorbed layer of 1 mM DDAB + 0.5 wt % D100 showing (a) the layer furthest from the mica surface and (b) the film closest to the mica surface. Representative height profiles of each layer on the same scale as the deflection images clearly show the greater roughness in the outer layer.

was imaged at a force corresponding to the layer closest to the mica surface (separation ~ 2.4 nm). Both these images are featureless with the outer layer noisier than the inner, as can be assessed from the corresponding height profiles. Images captured in which drift in the applied force caused the tip to rupture the outer layer measured a push-through distance of approximately 2.8 nm. This agrees well with the data from the force curve.

Surface Forces Apparatus: Normal Interaction Forces. Interaction force curves between mica surfaces immersed in DDAB/D100 solutions were measured with the SFA. Unlike the AFM, in this experiment, the interaction force between identical macroscopic mica surfaces is measured in symmetric conditions. Representative curves of the measured interaction force normalized by the local radii of curvature of the mica surfaces are presented in Figure 4, where the position $D = 0$ was determined with the mica surfaces in contact immersed in distilled water. In general, the force profile between the mica surfaces in a solution of 1 mM DDAB is similar to those reported previously for other double-chained bilayer-forming surfactants when the bulk concentration is above the cmc.[23] At large separation between the surfaces, an electrostatic repulsion between the charged

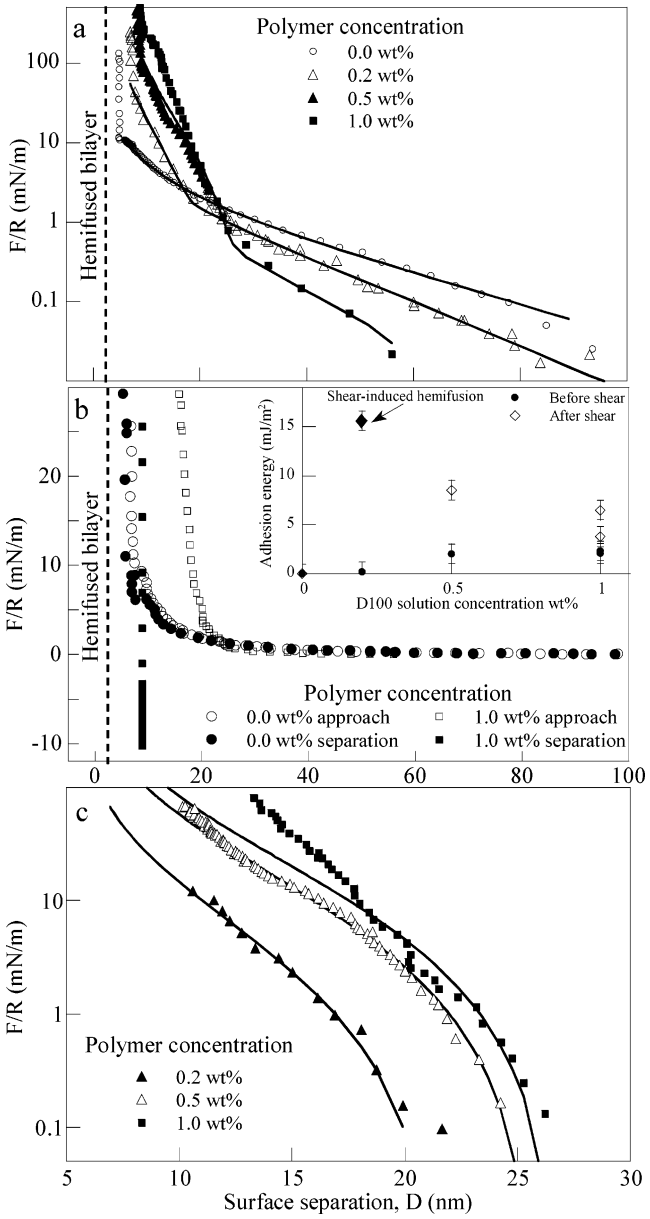

Figure 4. (a) Normal force profile between two mica surfaces in a solution of 1 mM DDAB and various polymer concentrations. The solid lines correspond to the theoretical interaction curve, as described in the text. (b) Normal force profile between two mica surfaces in a solution of 1 mM DDAB in the absence or presence of D100 shown on a linear scale, to highlight the attractive interaction. Inset: adhesion energy between the surfaces measured from the pull-off force as a function of polymer concentration before (closed circles) and after (open diamonds) shearing the surfaces in contact. The enhanced adhesion observed at 0.2 wt % D100 is due to the shear-induced hemifusion of the bilayers. (c) Steric component of the interaction force obtained by subtracting the DLVO interaction force from the total measured force. The solid lines correspond to the best fit to the Alexander−de Gennes model.[26]

Table 2. Parameters Derived in the Theoretical Fit to the Measured Force Profiles Shown in Figure 4: Debye Length (κ^{-1}), Interaction Hard Wall Distance (HW), Surface Charge Density (σ), Distance between Grafting Sites (s), Chain Extension (L), and Thickness of Adsorbed Surfactant Layer That Determines the Zero Distance for the Brush−Brush Interaction (T)[a]

				s (nm)		L (nm)		
copolymer loading (wt %)	HW (nm)	κ^{-1} (nm)	σ (C/m^2)	force	adsorption	force	adsorption	T (nm)
0	5	20.9	0.020					
0.2	5.5	15.1	0.013	4.0	3.4	8.3	8	2.5
0.5	8	14.0	0.011	3.2	1.8	10.4	12	2.5
1.0	8.5	10.5	0.0065		1.0		18	

[a] Also shown for comparison are s and L derived from adsorption isotherm measurements.

bilayers is observed. When the adsorbed bilayers approach, a hydration force barrier that deviates from the prediction of the DLVO theory can be observed for separations less than 7 nm. Neither the hemifusion nor the desorption of the adsorbed bilayers of DDAB could be induced by increasing the pressure, even at the highest normal pressures accessible (on the order of 10 MPa). Similar results were reported previously by Boschkova et al.[24]

Increasing polymer concentration reduces the magnitude of the long-range electrostatic repulsion between the surfaces, indicating a reduction in the charge density on the adsorbed bilayers. The anchored polymer molecules also introduce an intermediate-range repulsion observable at surface separations less than 25 nm. The electrostatic repulsion contribution to the interaction force profile disappears or is very small for 1.0 wt % D100, indicating that the surface charge density under these circumstances is substantially reduced. Similar effects were reported for D100 incorporated into a DTAB surfactant layer on mica.[13]

The high repulsive wall is progressively displaced from 5 nm in pure DDAB to larger separations with increasing polymer concentration, reaching 8.5 nm for 1.0 wt % D100. Just as for the pure DDAB solution, under no circumstance were we able to induce hemifusion between the mixed adsorbed layers *by compression alone*. This can be seen from the measured separation between the surfaces under high compression. The displacement of the position of the repulsive wall indicates that diblock molecules remain trapped in the contact area when the surfaces are compressed. However, through *the combined effects of shear and compression*, the separation of the surfaces can be further decreased, and removal of the diblock molecules from the contact area and even hemifusion of the adsorbed bilayers may be attained, as discussed in the next section.

The force profile, $F(D)$, measured between two cross-cylinders of radii R can be related to the interaction energy per unit area of two flat surfaces, $W(D)$, by using the Derjaguin approximation,[25] $F(D) = 2\pi RW(D)$. For the systems presented in this paper, two main components to the potential of interaction can be identified. First is the interaction between the charged layers, which can be described by the DLVO theory. This combines the electrostatic repulsion and the van der Waals attraction occurring between the charged surfaces.[25] The second component is the interaction between the physigrafted polymer brushes, which can be modeled by the Alexander−de Gennes theory.[26] For cylindrical surfaces of radius R, this theory predicts

$$F(D)/R = \frac{16KT\pi L}{35s^3}\left[7\left(\frac{2L}{D}\right)^{5/4} + 5\left(\frac{D}{2L}\right)^{7/4} - 12\right], \quad \text{for } D < 2L$$

where L is the brush thickness and s is the distance between grafting sites.[27] This equation combines the osmotic repulsion between grafted coils, and the reduction of the elastic energy on the chains as they are compressed.

The measured data were fitted assuming that the above-mentioned two components to the interaction potential are simply additive. The electrostatic component was determined by fitting the measured force data at long distance. The excess of the measured force over the prediction of the nonlinear Poisson−Boltzmann equation at short separations was then attributed to the steric interaction. A summary of the parameters that produced the best fit of the experimental results is presented in Table 2. It was consistently observed that assuming boundary conditions of constant surface charge produced a better fit of the data, as has been reported before.[23,27] In all cases, the plane of charge was placed at the position of the repulsive hard wall force. The surface charge obtained for the DDAB bilayer (0.020 C/m^2, corresponding to 0.12 elementary charge per square nanometer) indicates that the charge of more than 90% of the adsorbed molecules is neutralized by bounded counterions (assuming a headgroup area of 0.6 nm^2).[28] It was also observed that the decay length of the electrostatic repulsive force (Debye length, κ^{-1}) is larger than the value predicted by the ionic strength of the solution. However, assuming that only 25% of the DDAB molecules on the micelles are dissociated, as suggested first by Pashley and Ninham,[29] a value of 19.5 nm can be estimated for κ^{-1}, in good agreement with our experimental result. All these features are similar to what has been reported before for other charged surfactant layers interacting in solution.[23] In addition, the characteristic decay length of the electrostatic repulsion decreases with polymer concentration, which may be an indication of increasing concentration of free bromide counterions in solution, as a consequence of the formation of mixed copolymer−surfactant micelles.

The solid lines in Figure 4a represent the best fit to the experimental data of the combined interaction energy. In Figure 4c the second contribution to the measured force is presented. For this figure the experimental data points were obtained by subtracting the fitted DLVO force from the measured total force, and the solid lines correspond

(23) McGuiggan, P. M.; Pashley, R. M. *J. Colloid Interface Sci.* **1988**, *124*, 560.
(24) Boschkova, K.; Kronberg, B.; Stalgren, J. J. R.; Persson, K.; Salagean, M. R. *Langmuir* **2002**, *18*, 1680.
(25) Israelachvili, J. *Intermolecular and Surface Forces*, 2nd ed.; Academic Press: New York, 1991.
(26) de Gennes, P. G. *Adv. Colloid Interface Sci.* **1987**, *27*, 189.
(27) Kuhl, T. L.; Leckband, D. E.; Lasic, D. D.; Israelachvili, J. N. *Biophys. J.* **1994**, *66*, 1479.
(28) Brady, J. E.; Evans, D. F.; Warr, G. G.; Grieser, F.; Ninham, B. W. *J. Phys. Chem.* **1986**, *90*, 1853.
(29) Pashley, R. M.; Ninham, B. W. *J. Phys. Chem.* **1987**, *91*, 2902.

to the best-fit values of the variables s and L. As can be observed, there is reasonably good agreement between the experimental data and the predictions of the theory, except at the highest concentration of polymer investigated. The position for the zero distance for the brush−brush interactions was considered to be at the thickness of a surfactant bilayer (2.5 nm per surface).

The addition of the diblock copolymer also substantially modifies the forces between the surfaces upon separation, in a way that is not predicted by the theories mentioned above (Figure 4b). Two polymer concentration regimes can again be distinguished, for polymer concentrations less than or greater than about 0.4 wt %. They correspond to the same regimes already noticed during the AFM study, which will again be identified in the discussion of the behavior under shear.

While the force profile measured with DDAB alone is virtually reversible during a loading−unloading cycle, the addition of D100, at concentrations greater than 0.4 wt %, induces an attractive component in the force profile, as shown in Figure 4b. The corresponding adhesion energy as a function of the polymer concentration, determined from the pull-off force, is presented in the inset of this figure. This additional attraction is observed only if the surfaces are brought closer than 11 nm before separating; otherwise, the measured force profile is completely reversible. It is important to emphasize that this adhesion is not related to hemifusion of the adsorbed layers: it occurs at separations larger than 6.5 nm, larger than the thickness of two adsorbed monolayers. A similar increase in adhesion energy with increasing D100 grafting density was reported by us for the cationic trimeric surfactant 12-3-12-3-12.[15] The measured adhesion energy was not affected either by time under compression or by the normal force applied before separating the surfaces. However, a substantial increase in the measured pull-off force was observed if the surfaces were sheared before separation.

For polymer concentrations less than 0.4 wt % no significant adhesion is measured between the mixed adsorbed bilayers. On the other hand, on certain occasions hemifusion may be shear-induced (see below). Under such circumstances the corresponding adhesion energy is much larger than that measured at higher polymer concentrations in the nonhemifused state, as shown in the inset of Figure 4b for 0.2 wt % D100.

Surface Forces Apparatus: Behavior under Shear. As mentioned above, we do not detect any frictional resistance when adsorbed bilayers of DDAB are sheared at any applied velocity or normal load. We have observed a similar behavior several times before with other self-assembled bilayers of charged surfactants on mica, as long as the bilayers remain intact under compression and shear—that is, as long as the adsorbed bilayers do not hemifuse.[4−6,15] However, unlike other surfactants we have studied in the past, it was impossible to induce hemifusion of the adsorbed DDAB bilayers. At the bulk concentration of 1 mM used in this study, at which the DDAB molecules self-assemble in bulk solution to form vesicles, the DDAB adsorbed bilayers retained their superior lubricant properties independent of the time under shear and whatever normal load we were able to impose. From the measured area of contact between the compressed surfaces, it can be inferred that the shear stress between the bilayers was lower than 5 kPa at the highest normal loads investigated. This value can be compared with the typical measured shear stress after hemifusion has occurred, on the order of a few hundred kilopascals.

A more complicated scenario was observed after grafting D100 molecules onto the adsorbed DDAB layers. Depending on bulk polymer concentration, and consequently on the amount of grafted D100, the two concentration regimes previously noticed are again distinguished:

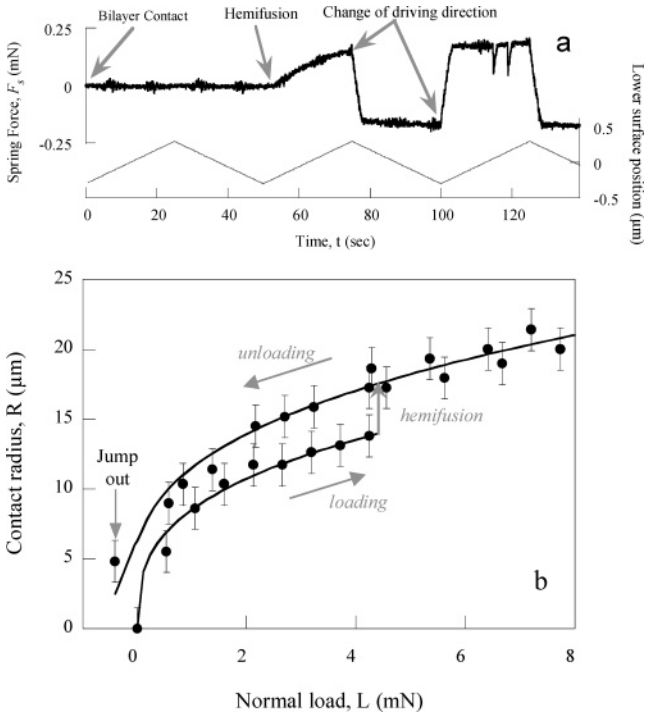

Figure 5. (a) Friction signal recorded at the moment of shear-induced hemifusion for 0.2 wt % D100. Driving velocity 24 nm/s, normal load 4.5 mN. A dramatic increase in friction force is accompanied by a film thickness reduction from 6.5 nm to 3.5 nm, indicating the hemifusion of the adsorbed bilayers. Two isolated stick−slip events can be observed at about 120 s, indicating the proximity to the smooth-sliding/stick−slip dynamic transition. (b) Variation of the contact radius, R_c, with applied normal load for mica surfaces immersed in 1 mM DDAB and 0.2 wt % D100. The solid lines correspond to the best fit of the data to Hertz (before the hemifusion) or JKR (after the hemifusion) models of contact mechanics.[1] The lower surface was driven at 24 nm/s during the loading−unloading cycle. After the hemifusion the surfaces becomes adhesive and are able to sustain a negative load before jumping apart.

(i) Polymer Concentrations < 0.4 wt %. As observed with DDAB alone, no measurable friction force could be detected when the surfaces were sheared under compression along the repulsive hydration wall. Despite the fact that adding D100 increases the repulsive force between the surfaces, this addition makes it possible to induce the hemifusion of the adsorbed layers by the combined effect of shear and compression. Under these circumstances, a transition occurs from a nonhemifused state of extremely low friction with the surfaces separated 6.5 nm to a hemifused state of high friction with a larger flattened contact area and the surfaces 3.5 nm apart. This is illustrated in Figure 5a, where the dramatic increase in the measured friction force accompanying hemifusion can clearly be observed. This result suggests that the lateral cohesiveness of the adsorbed film is altered in the presence of D100. Shear-induced hemifusion can also be followed by measuring the deformation of the contacting surfaces under the applied load. This is presented in Figure 5b, where the radius of the flat circular area between the two compressed surfaces under shear is shown as a function of the applied normal load. For adsorbed DDAB bilayers, no hysteresis along a loading−unloading cycle is observed, and the results measured in both cases are almost identical. The elastic deformation of the surfaces in this case can be described by Hertz theory,[1] well suited to account for

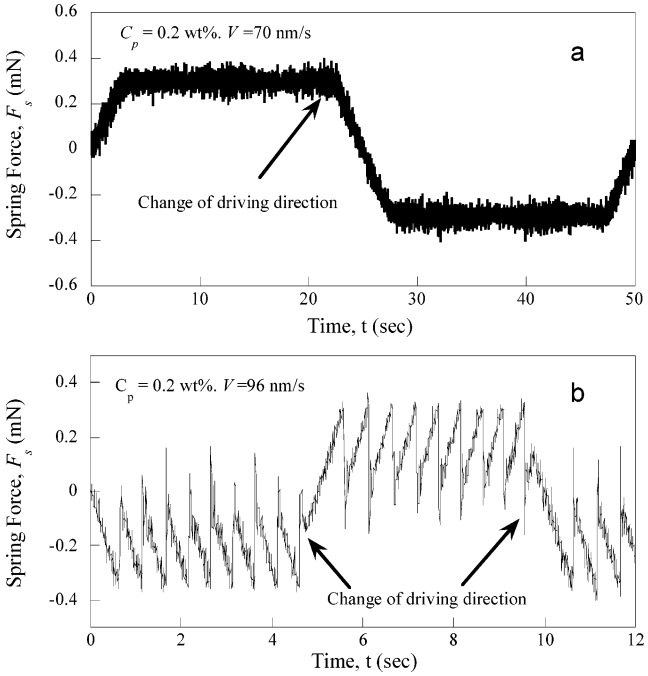

Figure 6. (a) Smooth sliding regime of constant spring force observed at low driving velocities, $V < V_c$. (b) In the stick−slip regime ($V > V_c$) the measured spring force oscillates between two kinetic values. On the slip events, the spring can deflect beyond the zero force value, indicating underdamped conditions of the spring-mass system.

nonadhesive contacting surfaces under pressure. When D100 is introduced into solution, before hemifusion of the bilayers is induced by shearing, the radius of the contact area versus the load also follows a Hertz profile. Once the hemifusion transition has occurred, it is better described by the JKR theory for the contact of adhesive surfaces[1] down to the contact rupture, as shown in Figure 5b. The load necessary to induce hemifusion depends on the applied shear rate and the time the surfaces have been rubbed.

Once hemifusion has been achieved, the behavior of the surfaces under shear is similar to that observed with other adhesive boundary lubricated surfaces, as we have extensively described previously.[4−6] Several sliding regimes can be identified depending on the driving velocity. A regime of inverted stick−slip is present at intermediate driving velocities, while smooth sliding is observed at low velocities. The dynamic transition from smooth sliding to stick−slip response occurs at a well-defined driving velocity, known as critical velocity V_c. Typical friction traces for the two dynamic regimes observed are presented in Figure 6.

(ii) Polymer Concentrations >0.4 wt %. At higher D100 concentrations, the system exhibits a different behavior under shear. A measurable friction force is observed even without hemifusion, at separations as large as 9 nm at which the polymer-induced adhesion was measured. In this concentration regime, hemifusion was rarely observed even after a long time of shear at any applied load. Figure 7 shows the sliding curve for a polymer concentration of 0.5 wt % at different normal loads. Interestingly, the shear stress, σ, versus sliding velocity, V, curve is bell-shaped, similar to other adhesive, boundary lubricated surfaces under shear[4−6] and similar to the one measured here in the low polymer concentration regime with hemifused bilayers. Inverted stick−slip could also be observed above a critical velocity, V_c. At slower driving velocities, the measured shear stress appears to be independent of the

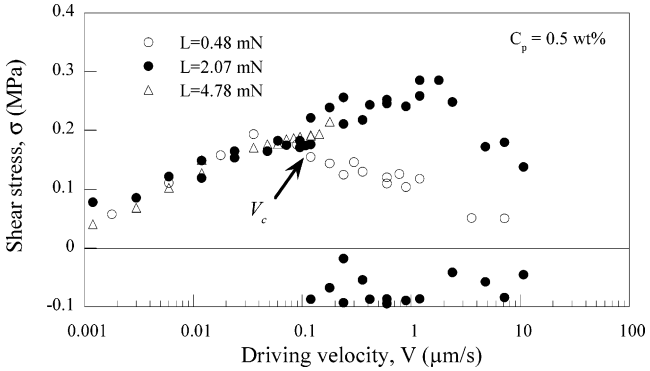

Figure 7. Driving-velocity dependence of the shear stress, measured at 0.5 wt % D100. The maxima and minima of the stick−slip oscillations are shown for normal load of 2.07 mN. The negative values of the measured force illustrate the possibility of overshooting on the spring deflection at the mechanical instability. For other normal loads the mean value of the measured spring force is shown when stick−slip was observed.

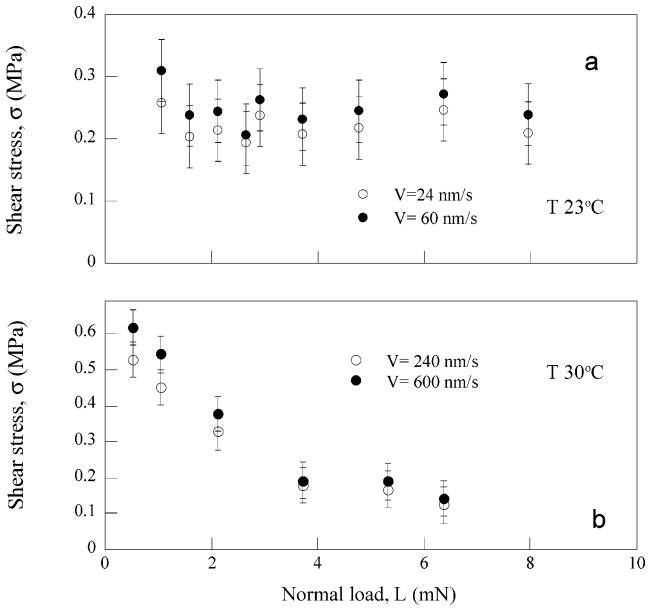

Figure 8. Load dependence of the measured shear stress at 1 wt % D100 and (a) $T = 23$ °C and (b) $T = 30$ °C, at driving velocities corresponding to the plateau of the sliding curve in each case, where smooth sliding is observed.

applied load, as shown in Figure 8a. The invariance of shear stress with applied normal load indicates that the frictional force is proportional to the area of contact between the two surfaces. In this concentration range, the surfaces could never be brought closer than 8.5 nm, indicating that a mixed DDAB−D100 layer remains trapped between the compressed surfaces.

A different response of the system was observed when the temperature was increased to 30 °C. By shear and compression the surfaces could be approached to 6.5 nm, corresponding to nonhemifused DDAB bilayers in contact. This suggests that the grafted diblock copolymer molecules could be either easily expelled from or rearranged within the contact area, suggesting a higher mobility of the D100 molecules at this higher temperature. Figure 8b shows how, at a higher temperature, the measured shear stress at the slower driving velocities preceding the stick−slip regime now decreases substantially when the normal load is increased. Nevertheless, the general sliding curve at any given load still shows a maximum value at V_c, as shown in Figure 9.

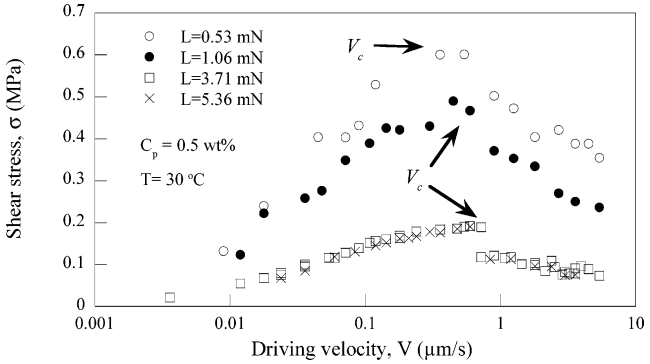

Figure 9. Driving-velocity dependence of the shear stress at $T = 30$ °C, measured at 1.0 wt % D100. When stick−slip was observed ($V > V_c$), the mean value of the measured spring force is presented.

Discussion

The incorporation of diblock copolymer into the adsorbed DDAB film is expected to occur via grafting of their hydrophobic blocks into the bilayer with the PEO chains left free in solution. All three techniques used to study the adsorbed film revealed the uptake of D100 into the bilayer with significant changes in the composition of the film and consequently in the film response to both applied normal loads and lateral shear. The adsorption study suggests that at low bulk polymer concentrations the original bilayers are decorated by anchored diblock chains, while at higher concentrations the modification is more significant since the coadsorption comes about with substantial desorption of surfactant molecules (see Figure 1). Surfactant desorption is further confirmed by the force profiles measured with the SFA (Figure 4 and Table 2) which show that the charge density due to the cationic surfactant decreases when the concentration of grafted polymer increases. However, for polymer concentrations up to 2 wt % no change in adsorbed film morphology was detected in the AFM images. Measurements at higher polymer concentrations similarly revealed no shape transitions, and these solutions were unstable and clouded over a period of 2 days. For D100 concentrations greater than 0.4 wt %, a second layer was seen to develop above the underlying DDAB bilayer. This second layer was only observed in experiments in which a tip with a spring constant less than 0.32 nN/m was used (long cantilever). When this same system was studied using a tip with a higher spring constant (short cantilever), the inner breakthrough was not observed at either polymer concentration of 0.5 or 1 wt %. Instead, the film was observed to thicken to a separation at breakthrough of approximately 5 nm (1 wt % D100) corresponding to the outer jump shown in Figure 2. The weaker spring is more force sensitive and could be held temporarily above the inner DDAB-rich bilayer while the stiffer tip ruptured both inner layer and outer layer simultaneously.

The lack of lateral structure change with addition of D100 may appear surprising, as the drive to avoid overlap of neighboring bulky EO_{100} headgroups should dominate at high D100 concentrations. In a previous study of mixed adsorption of DTAB and D100 on mica, it was reported that the amphiphilic diblock copolymer increased the curvature of the surface micelles, inducing a transition from rodlike to globular aggregates.[13] However, the bilayer formed by DDAB resists any change in morphology. As D100 does not itself adsorb to mica, any change in structure must be driven mainly through disruption to the packing of the outer layer. In a separate study[30] examining mixtures of DDAB with another adsorbing surfactant (DTAB), loadings in excess of 99 mol % were required to observe a nonbilayer adsorbed structure. Due to both the solubility limit of this copolymer and the minimum concentration of DDAB required to form a complete bilayer, this ratio could not be achieved in the present case. Such resistance to any change in morphology can certainly be attributed to a high degree of order of DDAB molecules in the inner monolayer directly adsorbed onto the smooth mica surfaces.

At low grafting density, the Flory radius, R_F, of the D100 headgroup can be calculated assuming good solvent conditions using $R_F = aN^{0.6}$, where a is the effective monomer length (Kuhn length = 0.35 nm for EO) and N is the number of monomers in a chain.[31] This yields a value of 5.5 nm for D100. If the mean separation between grafting sites is less than R_F, polymer chains start to interact, and the mushroom-to-brush transition occurs.[32] From the adsorption results in the absence of D100, and assuming an area per DDAB molecule, A_{DDAB}, of 0.6 nm^2,[28] the specific surface area of the ground mica for DDAB adsorption, s_a, can be estimated as s_a = (11.5 μmol of DDAB/g of mica)(N_{Av})(A_{DDAB})/2 = 2.1 m^2/g, where N_{Av} is Avogadro's number and the factor of 2 takes into account the fact that DDAB adsorbs in the form of bilayers. On the basis of this result and the R_F value determined above, it can be estimated that the grafted D100 molecules start to overlap when the amount of D100 adsorbed exceeds 0.15 μmol/g. This indicates that substantial interaction between grafted D100 chains occurs even at the lowest polymer concentration investigated by us (0.2 wt %, Figure 1). Nevertheless, at this polymer concentration, the D100 molecules under the approaching AFM tip are still capable of lateral movement, and no discrete outer layer is observed (Figure 2). The lateral mobility of the grafted diblock molecules is further confirmed by the hard wall separation measured with the SFA: at a polymer concentration of 0.2 wt % the mica surfaces can be brought under strong compression to separations similar to those for DDAB alone. The measured deflection of the AFM cantilever at breakthrough of the inner layer is at its maximum at this D100 grafting density, due to the combined effect of the electrostatic repulsion between the charged bilayers, which are still rich in charged DDA^+ ions, and the steric repulsion between grafted polymer layers due to excluded volume effects.

At polymer concentrations greater than roughly 0.4 wt %, the formation and growth in strength of the outer layer suggests the bulky headgroups are being forced into a more extended configuration, as a mushroom-to-brush transition has already taken place. As the AFM tip approaches this dense PEO layer, it is deflected at distances as far as 15−20 nm from the surface. With a reduction in separation, the cantilever is further deflected and the layer compressed up to a breakthrough at a tip−surface separation of 5 nm. Because the D100 headgroups are so densely packed, their ability to swiftly migrate laterally away from the region of the tip is limited and consequently the film ruptures at higher applied force. This is consistent with the higher concentration of D100 in the adsorbed layers, the thicker hard wall measured with the SFA, and the impossibility of inducing the

(30) Blom, A.; Duval, F. P.; Kovacs, L.; Warr, G. G.; Almgren, M.; Kadi, M.; Zana, R. *Langmuir* **2004**, *20*, 1291.
(31) Flory, P. J. *Statistical Mechanics of Chain Molecules*; Wiley-Interscience: New York, 1969.
(32) Milner, S. T. *Science* **1991**, *251*, 905.

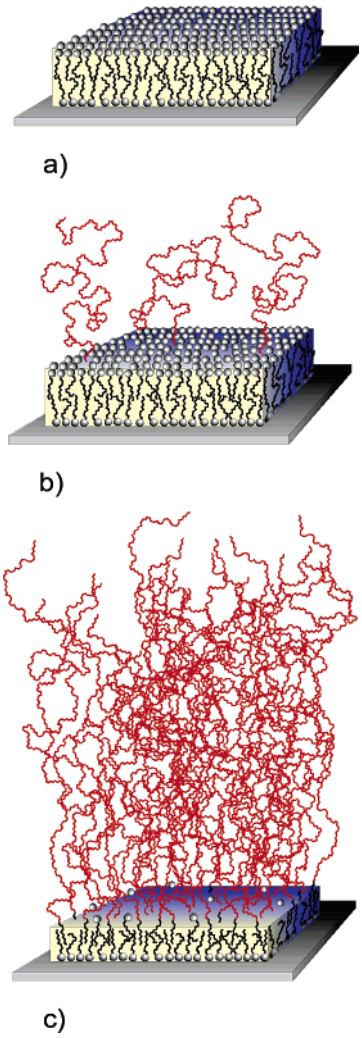

Figure 10. Schematic representation of mixed adsorbed layer. (a) DDAB; (b) 0.1 wt % D100; (c) 0.5−1.0 wt % D100. At low polymer concentrations (b), there is little intermolecular interaction between adsorbed D100 molecules. The tethered polymer adopts a mushroom conformation. At higher grafted densities (c), the chains are more constrained and are forced into a brushlike conformation.

hemifusion of the mixed adsorbed layers under shear and compression.

The mean separation between tethered D100 chains, s, can be calculated from the measured adsorbed layer compositions. The extension of the brush, L, can then be estimated by using $L \approx s(R_F/s)^{5/3}$.[33] The values obtained by this calculation are shown in Table 2 alongside the values obtained from fitting the SFA force profiles. The agreement between the two sets of values is significant, considering that they are obtained by using two very different techniques and that D100 is a polydisperse sample. The density of grafted chains calculated from the SFA force profiles seem to be consistently smaller than the values measured from the adsorption experiments. This may reflect the mobility of the grafted chains on the surface. Increasing the normal pressure between the surfaces may force some chains to quit the contact region, effectively reducing their density. Configurations of the mixed adsorbed film at 0.2 and 1 wt % D100 are represented schematically in Figure 10.

At 2 wt % D100, the surface contains 49 mol % D100 and no inner layer is observed with the AFM. This is due both to weakening of the underlying surfactant film as DDAB monomers are replaced by D100 and to strengthening of the outer EO-rich layer. The value of 49 mol % D100 for the entire adsorbed film equates to about 90 mol % D100 in the outer layer of the film. Thus, at this concentration the outer surfactant monolayer of the initial bilayer has almost disappeared completely, and is replaced by diblock chains anchored into the adsorbed surfactant monolayer. A likely consequence is that the lateral migration of compressed chains is more restricted through this adsorbed monolayer. The force at which the tip penetrates the adsorbed film is greater than the force required previously at all polymer concentrations.

The changes in the structure of the DDAB film induced by D100 coadsorption have direct implications on the behavior of the surfaces under shear. Two main effects can be identified depending on the polymer grafting density.

At low polymer concentrations, the incorporation of grafted copolymer molecules seems to reduce the lateral cohesiveness of the adsorbed film, allowing the hemifusion of the adsorbed layers under shear, which was impossible to achieve between bilayers of DDAB alone. This is not in contradiction to the enhanced compressibility modulus of the adsorbed layer observed at low polymer concentrations. The presence of the D100 molecules increases the repulsion between the adsorbed layers by steric interactions. However, in this low grafting density regime the D100 chains, which are mainly anchored into the outer surfactant monolayer, may migrate laterally under compression to relieve the constraint. As a consequence of this migration, the outer monolayer in the compressed zone is now less dense than a complete monolayer obtained in a pure DDAB solution. The outer monolayers then contain defects that are good sites for the nucleation of the hemifusion process. The same behavior is observed with adsorbed surfactant bilayers when the bulk concentration is reduced below the cmc where hemifusion is easily achieved between the incomplete bilayers. In contrast, above the cmc the complete bilayers resist hemifusion.

At the higher densities of grafted D100, a new mechanism of dissipation of energy under shear emerged. High frictional forces between rubbing surfaces are detected even if hemifusion of the adsorbed layers is not attained. For the bilayer-adsorbing surfactants and surfactant−polymer systems we have studied in the past, hemifusion was a *sine qua non* condition for the observation of high friction forces.[4,15] This is not the case for the DDAB−D100 mixed layers. The invariance of the measured shear stress with the applied normal load (Figure 8a) and its bell-shaped sliding curve (Figure 7) as measured at 23 °C strongly resembles previous observations of weakly adhesive surfaces under shear.[4−6] At these high grafting densities the behavior of the mixed adsorbed films under shear appears to be adhesion dominated. This is consistent with the extra adhesion measured when the films are brought into contact, even though no hemifusion occurs.

Understanding the origin of this adhesion seems to be the key to understanding the behavior of these films under shear. Few studies of surface forces between grafted PEO chains have been published, and adhesive forces between layers of grafted PEO molecules are rare.[12,27] Raviv et al.[11] observed a small adhesion between grafted, $-N(CH_3)_3^+$-terminated PEO molecules and mica surfaces only at 0.1 M NaCl concentration, attributing it to bridging of the weakly adsorbing PEO chains between the surfaces. In our case, this scenario can be ruled out since the ionic strength fixed by the surfactant concentration is very

(33) Alexander, S. *J. Phys. (Paris)* **1977**, *38*, 983.

small. Sheth and Leckband[34] also observed a weak, specific adhesion between methoxy-terminated PEG chemically grafted onto a Langmuir−Blodgett lipid film and the protein streptavidin, adhesion that was not observed between either bare lipid and grafted PEG or two layers of grafted PEG. This was ascribed to attractions between certain low-polarity PEG conformers and hydrophobic regions of the protein.

Another possibility comes as a consequence of confinement effects. The main differences between coadsorbed or tethered polymers studied here and previous studies of grafted polymers relate to the mobility of the polymer molecules in the adsorbed layer and the higher grafting densities used in this study. This high grafting density is accompanied by desorption of DDAB, particularly from the outer monolayer of the initially formed bilayers. Under compression, the coadsorbed chains may migrate away from the contact region, leaving density defects in the outer layers. Local adhesive junctions may form between opposing surfaces either by hydrophobic interaction between the DDAB aliphatic chains of the underlying adsorbed monolayers, or possibly by hydrophobic interaction between low-polarity PEG chain conformers on one surface and exposed hydrophobic regions on the other. In either scenario the desorption of DDAB that accompanies D100 uptake is a crucial feature. Adhesions between hydrophobic defects is essentially the same mechanism as that invoked above to account for hemifusion at low grafting density. However, at higher grafting densities polymer migration is restricted by lateral interactions between adjacent chains, so some D100 chains remain in the contact region. This results in the increased film thickness when the adsorbed layers are brought into contact (8.5 nm instead of 5 nm with bare bilayers). The presence of these polymer chains increases the barrier to hemifusion over the whole contact area, preventing a connecting stalk from forming between the two films.

The contact region can then be described as two inhomogeneous films with defects and dense domains of confined polymers, as illustrated in Figure 10c. These domains may also form adhesive junctions with the opposing surface, since we know that the bulk polymer/surfactant solution becomes unstable above some D100 concentration. The size of any inhomogeneities must be below the spatial resolution of the MBI technique (on the order of a few microns), since the observed interference fringes do not reveal any discontinuities. Such a picture of the contact area, comprising microscopic adhesive junctions, is consistent with the adhesive model accounting for the shear stress response of the confined film with bell-shaped sliding curves and the independence of load at low temperature. The load dependence of the shear stress observed at 30 °C can be ascribed to the enhanced mobility of the D100 molecules, due to a reduction of the effective viscosity of the adsorbed layer. This facilitates a reduction in the density of D100 molecules in the contact region under compression. However, the picture of inhomogeneous mixed films induced by confinement still applies since the shear stress becomes load independent above some normal load (Figure 8b) and the bell shape of the sliding curves is maintained (Figure 9).

(34) Sheth, S. R.; Leckband, D. *Proc. Natl. Acad. Sci. U.S.A.* **1997**, *94*, 8399.

Conclusions

The behavior of polymer−surfactant mixed adsorbed layers on mica surfaces under shear and compression has been studied. We have shown that hydrophobically modified PEO polymer coadsorbs on the negatively charged mica surfaces in the presence of the cationic surfactant DDAB, yielding flat films with no lateral structure.

In the absence of added PEO copolymer, the DDAB molecules adsorb on the mica surfaces as a flat bilayer with high lateral cohesion. No hemifusion could be induced and no frictional force could be measured between DDAB-coated surfaces at any load or sliding velocity. These bilayers show superior lateral cohesion and lubricant properties.

In the presence of PEO copolymer, two regimes of concentration are distinguished. At low grafted copolymer density, the lateral cohesiveness of the boundary surfactant bilayers is weakened and hemifusion of bilayers can be achieved by combined shear and compression. A consequence of this change is the appearance of a measurable adhesion-dominated shear stress between the rubbing surfaces after the shear-induced hemifusion of the adsorbed layers occurs. The weakening of adsorbed layer cohesiveness is attributed to a reduction of the molecular density of outer monolayer in which some surfactant molecules are replaced by macromolecules that can migrate under mechanical constraint.

At higher PEO adsorption densities, the mixed adsorbed layer is significantly modified compared to bare surfactant bilayers, with many surfactant molecules replaced by diblock copolymer molecules. A short-range attraction emerges between the two mixed adsorbed layers, which is responsible for a nonnegligible shear stress measured between the sheared surfaces. The films are again very cohesive, but the superior lubricant properties are compromised. The extra adhesion is attributed to spatial fluctuations of density with nanodomains bridging the two films either by hydrophobic interaction or by confinement-induced phase separation.

All these observations may have important implications on the performance of PEO-based coatings in biomedical applications.

Acknowledgment. This work was supported by the bilateral agreement between the Australian Research Council and the Centre National de la Recherche Scientifique (CNRS/ARC), and by the NEDO International Joint Research Program. A.B. acknowledges receipt of a Henry Bertie and Florence Mabel Gritton Postgraduate Scholarship from the University of Sydney.

LA047878E